EphA4 deficient mice maintain astroglial-fibrotic scar formation after spinal cord injury

Julia E. Herrmann, **Ravi R. Shah**, **Andrea F. Chan**, and **Binhai Zheng**[*]
Department of Neurosciences, University of California San Diego, School of Medicine, 9500 Gilman Drive, MC 0691, La Jolla, California 92093, USA

Abstract

One important aspect of recovery and repair after spinal cord injury (SCI) lies in the complex cellular interactions at the injury site that leads to the formation of a lesion scar. EphA4, a promiscuous member of the EphA family of repulsive axon guidance receptors, is expressed by multiple cell types in the injured spinal cord, including astrocytes and neurons. We hypothesized that EphA4 contributes to aspects of cell-cell interactions at the injury site after SCI, thus modulating the formation of the astroglial-fibrotic scar. To test this hypothesis, we studied tissue responses to a thoracic dorsal hemisection SCI in an *EphA4* mutant mouse line. We found that *EphA4* expression, as assessed by β-galactosidase reporter gene activity, is associated primarily with astrocytes in the spinal cord, neurons in the cerebral cortex and, to a lesser extent, spinal neurons, before and after SCI. However, we did not observe any overt reduction of glial fibrillary acidic protein (GFAP) expression in the injured area of *EphA4* mutants in comparison with controls following SCI. Furthermore, there was no evident disruption of the fibrotic scar, and the boundary between reactive astrocytes and meningeal fibroblasts appeared unaltered in the mutants, as were lesion size, neuronal survival and inflammation marker expression. Thus, genetic deletion of *EphA4* does not significantly alter the astroglial response or the formation of the astroglial-fibrotic scar following a dorsal hemisection SCI in mice. In contrast to what has been proposed, these data do not support a major role for EphA4 in reactive astrogliosis following SCI.

Keywords

Spinal cord injury; Eph receptor; glial scar; fibrotic scar; astroglial response; meningeal cells; CNS repair

INTRODUCTION

The astroglial scar is considered one of the central targets for therapeutic manipulations in the treatment of spinal cord injury (SCI) (Silver and Miller, 2004). This glial scar is made up primarily of reactive astroglia, whose thick processes are interwoven around the area of the lesion (Fawcett and Asher, 1999), effectively isolating tissue damaged by the injury from nearby surviving, healthier tissue (Sofroniew, 2009; Voskuhl, et al., 2009). At the border of

[*]Correspondence to: Binhai Zheng, Ph.D. Department of Neurosciences University of California San Diego 9500 Gilman Drive, MC 0691 La Jolla, CA 92093-0691 USA Phone: (858) 534-5807 Fax: (858) 822-1021 binhai@ucsd.edu.

the reactive astroglia and the inner injured area (i.e. the lesion core, or epicenter) is a glia limitans-like structure that separates the astroglial scar from a fibrotic scar made mostly of fibroblast-like cells of the meningeal origin (referred to as meningeal fibroblasts below) (Shearer and Fawcett, 2001). This fibrotic scar, less extensively studied in the literature, appears to be associated with a dense collagen meshwork that may trap both axon growth inhibitory and stimulating factors (Klapka and Muller, 2006). Some of the components of the scar, such as proteoglycans, are thought to be detrimental to recovery after SCI because they can contribute to the inhibition of axonal regeneration (Shearer and Fawcett, 2001; Silver and Miller, 2004). However, suppressing glial scar formation has been shown to negate its beneficial healing effects such as restriction of inflammation and neuronal survival (Faulkner, et al., 2004; Herrmann, et al., 2008; Okada, et al., 2006). These results indicate that the astroglial scar, and perhaps more generally the lesion scar, cannot simply be categorized as beneficial or detrimental (Sofroniew, 2009). Understanding how specific signaling pathways are involved in specific aspects of astroglial and fibrotic responses to SCI will provide important insight into developing targeted therapeutic strategies.

The Eph family of receptor tyrosine kinases, and their ligands the Ephrins, play important roles in axon guidance in the developing nervous system, such as retinotectal topographic mapping (Cheng, et al., 1995), formation of the anterior commissure (Orioli, et al., 1996), and spinal motoneuron axon guidance (Wang and Anderson, 1997). Although Ephs are most well known for their roles during development, it has become increasingly clear that they are also expressed in the adult stage where they may serve a multitude of functions in physiology and disease (Pasquale, 2008). Relevant to this study, Ephs are expressed by neurons, astroglia and meningeal fibroblasts after SCI, making them potential candidates that may influence the outcome of SCI (Bundesen, et al., 2003; Goldshmit, et al., 2004; Irizarry-Ramirez, et al., 2005; Miranda, et al., 1999; Willson, et al., 2002; Willson, et al., 2003). EphA4, in particular, is expressed by astroglia, neurons and axons after SCI (Fabes, et al., 2006; Goldshmit, et al., 2004). Indeed, a previous study reported a lack of astrocytic gliosis following a lateral hemisection SCI in *EphA4* mutant mice as indicated by the blunted upregulation of the astrocyte marker glial fibrillary acidic protein (GFAP) (Goldshmit, et al., 2004). These results suggest that EphA4 is critically involved in the formation of the astroglial scar.

Axon guidance molecules have long been hypothesized to play a role in SCI, particularly in axon regeneration after SCI (Niclou, et al., 2006). In a candidate genetic screen for axon guidance molecules that may regulate corticospinal axon regeneration, we initially considered EphA4 as one of the more promising candidates because of its known role in corticospinal axon guidance during development. However, the altered trajectory of the corticospinal tract and the hopping gait in *EphA4* mutant mice (Dottori, et al., 1998; Leighton, et al., 2001) complicated both the anatomical and the behavioral analyses of this mutant following SCI (see discussion). We therefore focused our study on the roles of EphA4 in astroglial-fibrotic scar formation after a dorsal hemisection SCI by characterizing tissue response to injury in an *EphA4* mutant mouse line (Leighton, et al., 2001). If EphA4 plays a major role in astroglial response, *EphA4* mutant mice would be expected to exhibit a substantial alteration in GFAP upregulation and/or improper formation of the boundary between reactive astrocytes and meningeal fibroblasts at the injury site. We found that, in contrast with the published report using a lateral hemisection SCI (Goldshmit, et al., 2004), mice lacking EphA4 do not show a substantial reduction in SCI-induced GFAP expression, at least with the thoracic dorsal hemisection injury model employed here. Nor did we find overt alterations in the astrocyte – meningeal fibroblast boundary or other aspects of tissue responses associated with normal scar formation such as neuronal survival and restriction of inflammation.

MATERIALS AND METHODS

EphA4 mutant mice

The *EphA4* gene trap mutation (Leighton, et al., 2001) was backcrossed to C57BL/6 at least three times before intercrossing to obtain homozygous mutants. Adult female littermates aged 2-5 months (average age: 4 months, unless noted otherwise) were used in this study. Genotyping was performed on tail DNA with standard PCR protocols. All *EphA4* mutants exhibited a hopping gait. All experimental procedures were approved by the Institutional Animals Care and Use Committee at the University of California at San Diego.

Spinal cord injury surgeries

Dorsal hemisection was performed as described with minor modifications (Lee, et al., 2009; Zheng, et al., 2005). Briefly, mice were anesthetized with 4% Avertin (0.02 mL/g of body weight) via intraperitoneal injection. A laminectomy of the T8 (thoracic 8) vertebrae was performed and the dura was punctured bilaterally with a 30-gauge needle to facilitate the insertion of the points of micro-scissors to cut 0.8 mm into the spinal cord. Cuts were made across the dorsal portion of the spinal cord in thirds, and to ensure transection of the axons, a micro-knife was passed 0.8mm deep once in each direction across the cord. After hemostasis, the muscle layers and skin were sutured.

Post-operative care

Mice were given 0.5 mL saline (0.9%) and allowed to recover on a warm pad. Buprenex was administered twice daily for the first 48 hours post injury (0.1 mg/kg body weight). Baytril (Bayer) was administered once daily for five days post injury (0.02 mL of 1:10 diluted solution per mouse). Bladders were expressed twice daily for the duration of the 4 or 14 day survival period.

Tissue preparation

At the end of the survival period, mice were given an overdose of the anesthetic Nembutal, and were perfused transcardially with 4% paraformaldehyde in phosphate buffered saline (PBS). The brains and spinal cords were removed and post fixed in the same solution for 4 and 2 hours, respectively. To cryoprotect the tissue, the brains and cords were then placed in 30% sucrose for at least 48 hours. After embedding in OCT, the injured area was cut sagittally on a cryostat to a thickness of 20 μm. Brains were cut in 40 μm coronal sections.

Immunohistochemistry

Primary antibodies used were: rabbit anti-GFAP (1:500; Dako) for Western blot analysis, rat anti-GFAP (1:500; Zymed Laboratories) for immunohistochemistry (unless noted otherwise), rabbit anti-fibronectin (1:500, Chemicon), rat anti-CD45 (1:1000; BD Pharmingen), biotinylated mouse anti-neuronal specific nuclear marker (NeuN) (1:100; Chemicon), rabbit anti-β-galactosidase (1:2000; MP Biomedicals, Inc.), and chicken anti-β-galactosidase (1:500; Abcam). Fluorescent immunohistochemistry was performed using the following fluorophore-conjugated secondary antibodies: anti-rabbit Alexa 488 (1:500) and anti-rabbit Cy3 (1:1000), anti-rat 488 (1:500), anti-chicken Alexa 488 (all from Invitrogen). Streptavidin 488 (1:1000) or 546 (1:1000) (Invitrogen) was used to visualize the biotinylated primary antibodies. DAPI (or 4',6-diamidino-2-phenylindole, 0.1 mg/mL) was used as a nuclear counterstain. Bright field immunohistochemistry was performed using biotinylated secondary antibodies, biotin-avidin-peroxidase complex, and diaminobenzene as the developing agent (Vector Laboratories). Images of immunohistochemistry were taken with a Zeiss microscope in conjunction with Axiovision software.

Data analysis, quantification and statistics

All quantification was conducted by observers blind to the genotypes.

Delineation of astroglial/fibrotic scar area—Lesion edge was defined as the interface between the GFAP-negative/fibronectin-positive lesion core with the GFAP-positive/fibronectin-negative regions surrounding the lesion core. GFAP-negative tissue was defined as tissue that had little GFAP immunoreactivity with few GFAP-positive cells or processes (Plemel, et al., 2008). For the vast majority of the injuries, the GFAP-positive processes formed a roughly linear boundary between GFAP-positive and GFAP-negative regions. Fibronectin-negative tissue was defined as regions of tissue with little fibronectin immunoreactivity. Lesion borders were drawn based on images taken with a 20× objective lens.

Lesion size—The area of the GFAP-negative/fibronectin-positive region of the lesion core was outlined manually and measured as the lesion size using the NIH ImageJ analysis software package. To normalize against the variability in the size of the spinal cord, the lesion size was expressed as a percentage of the total area of a 1.5 cm long segment of the spinal cord centered at the injury site. One or two sections from a medial position were measured for each animal.

GFAP/fibronectin expression—Once outlined manually, GFAP-positive and fibronectin-positive areas were separately quantified as the percentage of pixels for GFAP or fibronectin immunoreactivity above a threshold level per unit area. The threshold value was set to include GFAP or fibronectin-positive signal and exclude background staining. Threshold values for a given section and stain remained the same throughout the study. The percentage of pixels per unit area was measured for a region extending from the previously defined lesion edge to a distance 100 μm away from the lesion core. This area is referred to as the lesion border. In addition, the percentage of pixels per unit area was measured for the largely GFAP-negative region (i.e. lesion core) inside the lesion border. This area is the same area measured in lesion size measurements.

Neuronal survival—Neurons were visualized using bright field NeuN immunohistochemistry. The number of neurons in the grey matter extending 1 mm in either direction from the lesion core was quantified using NIH ImageJ Analyze Particles function. Final counts were expressed as the number of neurons per unit area.

Macrophage density—Macrophage density was quantified using NIH ImageJ Cell Counter plug-in function. Macrophages were defined as rounded CD45-positive cells containing a dark outline of staining on the cell surface. The number of CD45-positive macrophages in a 1.5 mm long segment of the cord centered at the injury site. Results are expressed as numbers of macrophages per unit area.

Groups—EphA4 +/+, +/- and −/− mice were analyzed for the measures outlined above. EphA4 +/+ and +/- mice were not different from each other on any measure and were pooled as controls.

Statistical Analysis—Statistical analysis was performed using GraphPad Prism 4.0. T tests or two-way ANOVA were used as indicated.

RESULTS

Assessing EphA4 gene expression with a gene trap reporter before and after SCI

The *EphA4* mutant used in this study was derived from gene trap mutagenesis and exhibits a hopping gait and corticospinal tract recrossing defect (Leighton, et al., 2001) that are identical

to the phenotypes described for null mutants made by gene targeting (Dottori, et al., 1998). In addition, the gene trap mutant carries a β-galactosidase (referred to as β-gal below) reporter gene that can be used to track cell bodies expressing the *EphA4* gene (Leighton, et al., 2001). We thus used β-gal immunoreactivity in the mutant as a reporter to examine *EphA4* gene expression in the brain and spinal cord before and after SCI. We applied a dorsal hemisection model of SCI at thoracic level 8 (T8) because this model is compatible with assessing corticospinal axon regeneration (but see discussion) (Zheng, et al., 2006).

In the uninjured adult mouse spinal cord, β-gal expression co-localized predominantly with GFAP-positive cells (Fig. 1A). Fourteen days after SCI, β-gal expression in areas near the injury site similarly co-localized with GFAP-positive cells, albeit now hypertrophic and reactive in appearance (Fig. 1B). As a control, neither uninjured nor injured wild type mouse spinal cord exhibited β-gal immunoreactivity above background levels (Fig. 1C, D). A small subset of β-gal-positive cells were also immunoreactive for the neuronal marker NeuN in the grey matter of uninjured EphA4−/− mouse spinal cord either before or after SCI (Fig. 2). Throughout layers II-VI of the sensorimotor cortex, β-gal expression co-localized with NeuN before and after SCI (Fig. 3A, B). Again, as a control, wild type mice did not express β-gal in the cortex before or after SCI (Fig. 3C, D). In both astrocytes and neurons, the scattered cytoplasmic β-gal staining pattern was consistent with what had been described for this particular gene trap reporter (β-gal preceded by a signal sequence and a transmembrane domain) (Leighton, et al., 2001;Skarnes, et al., 1995). Together, these results were consistent with previous reports that EphA4 is expressed on astrocytes, in neurons throughout the cortical layers and some spinal neurons following SCI (Cruz-Orengo, et al., 2006;Fabes, et al., 2006;Goldshmit, et al., 2004); however, with the β-gal reporter, astroglial expression of the *EphA4* gene is detected more readily in the intact spinal cord in our study.

Similar GFAP expression at the injury site in EphA4−/− and control mice after SCI

Since *EphA4* is mainly expressed by astrocytes in the injured spinal cord, we wanted to examine whether a lack of EphA4 would affect astroglial responses after SCI. One salient feature of reactive astrogliosis is an up-regulation of GFAP expression (Norton, et al., 1992). To determine if GFAP expression is altered in EphA4−/− mice in comparison to controls after SCI, we first performed Western blot analysis on protein extracts from a 1.5 mm segment of the thoracic spinal cord containing the lesion site 4 days after a dorsal hemisection SCI. The level of GFAP protein in the injured cord appeared comparable between *EphA4* mutants and heterozygous controls (Fig. 4A). Quantitative analysis of the Western blots did not reveal any statistically significant difference in GFAP expression levels between EphA4−/− and control mice before or 4 days after SCI (Fig. 4B). Both the mutants and the control mice exhibited a trend for increased EphA4 protein levels 4 days after SCI, but this trend did not reach statistical significance in either genotype likely due to the presence of a relatively large GFAP-negative area that develops at the injury site in mice.

We next used immunohistochemistry to further examine the possibility of more subtle differences in astroglial scar formation. We examined GFAP immunoreactivity at 4 and 14 days after a dorsal hemisection SCI in order to span different phases of the astroglial response to SCI. Previous studies indicated that at 4 days post SCI, the astroglial scar is not fully formed, and inflammation and cell death is high (Grossman, et al., 2001; Liu, et al., 1997; Norenberg, et al., 2004). As expected, in control mice, a dense network of GFAP-positive astroglial processes isolating the lesion core from the surrounding tissue was not fully formed at this time point (Fig. 5A). At higher magnifications, it appeared that GFAP-positive astrocytes had started to elongate but were either disoriented or perpendicular to the border of the injured area, forming a relatively loose network (Fig. 5C). The lesion core in control mice was characterized by GFAP-positive broken processes and debris (Fig. 5E). At a distance away from the injury

(e.g. ~400 μm), GFAP-positive cells could be discerned, where their cytoplasm and processes were not characteristic of hypertrophic astrocytes (Fig. 5G).

In EphA4−/− mice, at 4 days after SCI, we observed a similar pattern of GFAP expression in the lesion border. The GFAP-positive processes had not yet formed a dense meshwork around the injury (Fig. 5B). Closer inspection of the lesion border indicated a relatively loose network of GFAP-positive cells, either disoriented or perpendicular to the lesion edge (Fig. 5D) in a manner similar to controls (Fig. 5C). The lesion core in EphA4−/− mice was characterized by debris and broken processes (Fig. 5F) just as in control mice (Fig. 5E). Astrocytes in EphA4 −/− mice at ~400 μm away from the immediate injury site appeared similar to those of control mice, with relatively short GFAP positive processes (Fig. 5H).

In addition to these qualitative observations, we quantified the density of GFAP-positive pixels in the lesion border, defined as the area starting from the outer edge of the largely GFAP-negative lesion core to 100 μm outward into the surrounding tissue (Fig. 7A, outlined with solid white line). We chose this 100 μm-wide border for quantification because it appeared to encompass the majority of the thickest astroglial scar network following a dorsal hemisection. We also quantified the density of GFAP expression in the lesion core, defined as the central, largely GFAP-negative area (Fig. 7A, striped area). We found no statistically significant difference between groups in percent GFAP immunoreactivity in the 100 μm-wide lesion border or the lesion core 4 days after SCI (Fig. 7B).

At 14 days after SCI, in control mice, a clear border between the central core of unhealthy tissue/invading cells and surrounding surviving tissue had been formed by a dense network of GFAP-positive, reactive astrocytic processes (Fig. 6A) (Faulkner, et al., 2004;Norenberg, et al., 2004). Higher magnification view of the lesion edge revealed defined boundaries between the largely GFAP-negative lesion core and the GFAP-positive lesion border, and that the GFAP-positive reactive astrocytes had clearly oriented themselves in parallel to the lesion edge and formed a dense network made out of their enlarged processes (Fig. 6C). The lesion core was largely devoid of GFAP-positive cells (Fig. 6E). At ~400 μm away from the lesion edge, GFAP positive astrocytes did not appear hypertrophic (Fig. 6G).

In EphA4−/− mice at 14 days after injury, clearly defined borders were also observed, separating the central lesion core from the surrounding tissue (Fig. 6B). Closer examination of these borders also revealed that the astrocytes were similarly oriented running parallel to the central lesion core, forming a network of thickly intertwined processes (Fig. 6D). As in control mice, the lesion core was largely devoid of GFAP processes (Fig. 6F). Reactive astrocytes at ~400 μm away from the lesion core also appeared to have relatively short processes similar to those in control mice (Fig. 6H). Again, in quantitative analysis, we did not find statistically significant differences in percent area of GFAP immunoreactivity in the 100 μm-wide lesion border or the lesion core at 14 days after SCI (Fig. 7C, D).

Similar fibronectin expression at the injury site in EphA4−/− and control mice after SCI

In addition to GFAP-positive astrocytic processes bordering the lesion core after SCI, the lesion core becomes filled with invading meningeal fibroblasts, inflammatory cells and extracellular matrix molecules such as fibronectin and chondroitin sulfate proteoglycans (Fitch and Silver, 2008; Herrmann, et al., 2008; Ma, et al., 2001; Shearer and Fawcett, 2001; Wang, et al., 1997). To further examine characteristics of lesion scar formation and tissue response in EphA4 −/−mice, we examined fibronectin immunoreactivity in the lesion core and border, in the same manner as described for GFAP immunoreactivity above. Four days after SCI in control mice, the lesion core had largely been filled with fibronectin (FN)-positive cells and extracellular matrix (Fig. 8A), and some fibronectin immunoreactivity was found intermingled within the lesion border areas containing dense GFAP immunoreactivity (arrows in Fig. 8C). This result

is in agreement with published studies with a transection model in rats (Bundesen, et al., 2003). At 4 day after SCI in EphA4−/− mice, the fibronectin-positive cell/matrix similarly filled the center of the lesion and showed some intermingling with GFAP-positive cells (Fig. 8B, D). There was no statistically significant difference between the mutants and controls in the percent of fibronectin immunoreactive area in the lesion core or in the 100 μm-wide lesion border as defined above (Fig. 10A).

At 14 days after SCI, the astroglial scar was fully formed and lesion borders were distinct in control mice (Fig. 9A, C), again similarly as described for a transection injury in rats (Bundesen, et al., 2003). The largely GFAP-negative lesion core at 14 days after SCI appeared more compact compared to that at 4 days (compare to Fig. 8A). The morphology and density of fibronectin-positive cells/matrix in the lesion core appeared comparable between EphA4−/− (Fig. 9B, D) and control (Fig. 9A, C) mice. Quantification of the density of fibronectin immunoreactivity in the lesion core or the lesion border did not show statistically significant differences between EphA4−/− and control mice. However, across both genotypes, there was an appreciable further increase in fibronectin immunoreactivity over time at the lesion core ($P = 0.02$, two-way ANOVA) and a corresponding trend for further reduction at the lesion border ($P = 0.08$, two-way ANOVA) (compare Fig. 10A and B). This quantitative observation likely reflected a less developed injury site at 4 days after SCI where there was more intermingling of GFAP-positive astrocytes and fibronectin-positive meningeal cells as compared with a more developed injury site at 14 days where there was a higher degree of segregation of the two cell types (compare Fig. 8A, B to Fig 9A, B).

Lesion size, neuronal survival and inflammation marker expression in EphA4−/− and control mice after SCI

After SCI, reactive astrocytes are instrumental in restricting lesion size (Faulkner, et al., 2004; Herrmann, et al., 2008). Previous studies indicate that cultured astrocytes from EphA4 −/− mice fail to migrate and fill a scratch wound (Goldshmit, et al., 2004), a characteristic that might lead to an alteration in lesion size in EphA4−/− mice *in vivo*. To further investigate this finding, we measured lesion size, defined as the area of the lesion that is largely GFAP-negative and fibronectin-positive (Fig. 11A, B), at 4 and 14 days after SCI. To control for variations in the size of the spinal cord, the areas measured (Fig. 11C, dashed white line) were normalized to the height of the spinal cord and expressed as a percentage of a defined area of the spinal cord (see Materials and Methods for details). We found no statistically significant differences in the percent lesion area between control and EphA4−/− mice at 4 and 14 days after SCI (Fig. 11D).

In addition to up-regulating expression of intermediate filaments such as GFAP and Vimentin, and interacting with extracellular matrix molecules to form the glial scar, reactive astrocytes also have a role in promoting neuronal survival after SCI (Brambilla, et al., 2005; Faulkner, et al., 2004; Herrmann, et al., 2008; Kuno, et al., 2006). We therefore examined whether deleting EphA4 led to a substantial change in local neuron numbers close to the injury site using NeuN as a neuronal marker at 14 days after SCI. Macroscopically, the amount of neuronal loss at the center of the lesion appeared to be similar between control (Fig. 12A) and EphA4−/− (Fig. 12B) mice, and so was the density of neurons in the surrounding grey matter. Quantitative analysis on NeuN-positive cells within 1 mm rostral and caudal to the lesion center revealed no statistically significant difference between control and EphA4−/− mice (Fig. 12C). As a control, uninjured mice also did not show a significant difference in NeuN-positive cell density in a comparable region of the cord between the two genotypes (Fig. 12C). As expected, both genotypes displayed a significant reduction in NeuN-positive cells at the injury site as compared to the respective uninjured controls ($P < 0.05$, two-tailed *t*-test).

To determine whether EphA4 deletion led to substantial changes in the inflammatory response, another important aspect of tissue responses after SCI (Sroga, et al., 2003), we examined CD45 immunoreactivity as a macrophage marker at the injury site. At 4 days after SCI, inflammation is widespread (Hausmann, 2003). By the 14-day time point after SCI, the astroglial scar will have largely contained the inflammatory response within the GFAP-negative area inside the lesion. As expected, the overall survey of the lesion area at 4 days after SCI showed a widespread presence of CD45-positive macrophages in both control and EphA4−/− groups (Fig. 13A, B). By 14 days after SCI, in control mice, the CD45 stained cells were largely confined to the immediate lesion area, with little penetration of macrophages in areas distal to the lesion core (Fig. 13C). This result is in agreement with previously published studies (Herrmann, et al., 2008). EphA4−/− mice showed a restriction of CD45 cells in a manner similar to controls (Fig. 13D). Some macrophages were present in the tissue surrounding the center of the lesion in both groups (arrows in Fig. 13E, F). To quantify any subtle differences between groups, we counted the number of CD45-positive macrophages within a 1.5 mm long segment of the spinal cord centered at the injury site. The density of CD45-positive macrophages in EphA4−/− mice at 4 or 14 days after SCI was not significantly different from that in controls (Fig. 13G).

DISCUSSION

Ephrins and Eph receptors have been extensively documented in cell-cell interactions in a variety of developmental processes as well as in physiology and disease (Pasquale, 2008). Their expression following SCI have made them attractive candidates as modulators of recovery and repair after SCI (Bundesen, et al., 2003; Irizarry-Ramirez, et al., 2005; Miranda, et al., 1999; Willson, et al., 2002; Willson, et al., 2003). EphA4, in particular, has been reported to be expressed in astrocytes and neurons after SCI and proposed to play a critical role in inhibiting axon regeneration and in mediating reactive astrogliosis that occurs after SCI (Cruz-Orengo, et al., 2006; Fabes, et al., 2007; Fabes, et al., 2006; Goldshmit, et al., 2004). However, in contrast to a previous study (Goldshmit, et al., 2004), our data do not support a major role for EphA4 in mediating reactive astrogliosis after SCI, at least in a thoracic dorsal hemisection model. Our analyses went beyond simple GFAP upregulation and encompassed the fibronectin-positive component of the scar (i.e. the fibrotic scar), the segregation of the glial scar and the fibrotic scar as well as lesion size, neuronal loss and inflammation. In the following, we discuss the presence of both the astroglial and the fibrotic component of the scar after SCI in mice. We then discuss the implications of our study on the role of EphA4 in the astroglial response and astroglial-fibrotic scar formation, and highlight the differences between the previous study (Goldshmit, et al., 2004) and our study that could account for the different experimental results.

The astroglial-fibrotic scar after SCI

The formation of a glial (or astroglial) scar for which reactive astrocytes constitute the major component is well established in the SCI literature (Fawcett and Asher, 1999). The glial scar is considered both as a physical and chemical barrier to axon regeneration. The glial scar secretes chondroitin sulfate proteoglycans (CSPGs), among other candidate molecules, that are inhibitory to axon regeneration (Davies, et al., 1999; Silver and Miller, 2004). Degradation of the glycosaminoglycan chains of the CSPGs with Chondroitinase ABC promoted regenerative responses of spinal axons and functional recovery after SCI (Bradbury, et al., 2002). However, despite the inhibitory nature of the glial scar, attempts to conditionally ablate reactive astrocytes or downregulate astroglial response led to the discovery that the glial scar also plays a critical, beneficial role after SCI, isolating the surviving CNS tissues from the injury epicenter and restricting the inflammatory responses in a wound healing process (Faulkner, et al., 2004; Herrmann, et al., 2008; Okada, et al., 2006). Thus, modulating specific

aspects or molecular pathways of the glial scar, rather than simply reducing glial scar formation, would be the ideal approach to negate its effect on axon regeneration.

In contrast to the glial scar, much less attention has been paid to the fibrotic scar. After experimental spinal cord injury in mice, a largely GFAP-negative lesion epicenter/core develops that is filled with fibronectin-positive cells/matrices. Sources for the GFAP-negative cells include meninges and the vascular and immune system (Ma, et al., 2001; Sroga, et al., 2003). These cells together with extracellular matrix make up the fibronectin-positive fibrotic scar, which is surrounded by the glial scar that is strongly GFAP immunoreactive. This glial-fibrotic scar configuration can be best appreciated in a penetrating SCI model (i.e surgical transection) in mice such as one presented in this study. However, it is also evident that a fibronectin-positive area containing cells/matrix develops after non-penetrating injuries such as a crush or contusion in mice (Ma, et al., 2001; Plemel, et al., 2008; Sroga, et al., 2003; Zhang, et al., 1996). We speculate that this fibronectin-positive scar component has been better appreciated in mouse models of SCI partly because of no or reduced lesion cavitation present at the injury site in mice (Inman, et al., 2002; Ma, et al., 2001; Plemel, et al., 2008; Sroga, et al., 2003; Zhang, et al., 1996). Nevertheless, a similar fibronectin-positive component of the lesion scar has been documented in rat models of spinal cord injury (Bundesen, et al., 2003; Shearer and Fawcett, 2001). Thus, after SCI in both rats and mice, two species used most extensively to model human SCIs, a fibronectin-positive fibrotic scar area at the lesion epicenter accompanies the surrounding astroglial scar. Strategies to modulate scar formation need therefore consider both the astroglial and fibrotic components of the scar. Both components may be protective as a wound-healing response to SCI while both may produce inhibitory molecules that contribute to the restrictive nature of the injured CNS.

EphA4 in SCI and astroglial-fibrotic scar

A previous study reported that EphA4 deficient mice exhibit reduced reactive astrogliosis, enhanced spinal axon regeneration and functional recovery after a lateral hemisection SCI (Goldshmit, et al., 2004). One important consideration in interpreting these data is the fact that *EphA4* mutants exhibit midline-recrossing defects of corticospinal axons and a hopping kangaroo gait, with the latter attributed to aberrant local circuitry of the central pattern generator in the spinal cord (Dottori, et al., 1998; Kullander, et al., 2003; Leighton, et al., 2001). Our unpublished data indicate that such developmental defects could significantly confound the anatomical and behavioral analyses of EphA4 germline mutants following SCI. In particular, because the trajectories of the corticospinal tracts significantly differ between *EphA4* mutants and controls, a direct comparison on axon regeneration after SCI cannot be made definitively. Aberrantly recrossed spinal axons in *EphA4* mutants may bypass a lateral hemisection and be misconstrued as regenerated axons. Even with a dorsal hemisection, the altered corticospinal axon trajectory in the mutants makes it difficult to be certain that any alteration, especially if subtle or modest, in axonal distribution after injury as compared to wild type controls is due to altered axon regeneration and not the altered axonal trajectory prior to injury. Regarding behavioral recovery, our *EphA4* mutants tend to exhibit lateral recumbency (lying on their side) following dorsal hemisection, making it virtually impossible to accurately assess their locomotor recovery (our unpublished observation). This lateral recumbency is associated with an impaired ability to right themselves after injury and is likely a reflection of their pre-injury locomotion deficit (hopping gait, thus lack of coordination) that is exacerbated by SCI. Further work is required to definitively assess the role of EphA4 in axon regeneration and functional recovery following SCI, which can be best evaluated using an inducible gene deletion system in mice (Herrmann, et al., 2009; Zheng, et al., 2006). In this regard, it is interesting to note that an EphA4 function blocking peptide has been shown to reduce retraction of corticospinal axons after SCI and enhance recovery, but local EphA4 antisense oligonucleotide treatment did not

enhance axon regeneration or locomotor recovery (Cruz-Orengo, et al., 2007; Cruz-Orengo, et al., 2006; Fabes, et al., 2007).

In this study, we focused on the role of EphA4 in reactive astrogliosis because this phenotype is presumably not confounded by germline gene deletion. We found that genetically deleting EphA4 does not lead to substantial changes in reactive astrogliosis as assessed by GFAP immunoreactivity. To determine whether the fibrotic scar formation is affected by EphA4 deletion, we also examined the fibronectin-positive lesion core. Neither the GFAP-positive glial scar nor the fibronectin-positive lesion core after dorsal hemisection in mice were significantly altered by EphA4 deletion. Other aspects of tissue responses to SCI at the lesion site such as lesion size, neuronal survival and inflammation marker expression were also not significantly altered in *EphA4* mutants. We therefore conclude that EphA4 does not play a major role in reactive astrogliosis or the formation of the astroglial-fibrotic scar after a dorsal hemisection SCI in mice. Ephrin-Eph signaling has been implicated in astrocyte-meningeal fibroblast interaction at the injury site that help shape the glial-fibrotic scar (Bundesen, et al., 2003). Our results do not support a major role for the promiscuous EphA4 in this particular aspect of cell-cell interactions following SCI.

Our study is consistent with two published studies reporting no major alterations in reactive astrogliosis after treatment with either EphA4 function blocking peptide following a T10 contusion injury or antisense oligo-mediated reduction of *EphA4* gene expression following a C5 partial surgical transection in rats (Cruz-Orengo, et al., 2006; Fabes, et al., 2007). However, it is in contrast with a previous genetic study in mice that indicated a significant role for EphA4 in the astroglial response (Goldshmit, et al., 2004). Here we discuss the differences between the previous study and our study that could lead to the different experimental results.

Our study stemmed from our interest in the role of axon guidance molecules in CNS repair after spinal cord injury (Yaron and Zheng, 2007) and was not intended to be an exact replicate of the previous study (Goldshmit, et al., 2004). Thus, there are many variables between our study and the previous study. First, the two studies used different GFAP antibodies for immunohistochemistry. While Goldshmit used the rabbit anti-GFAP antibody (DAKO), we used a rat anti-GFAP antibody (Zymed) in order to perform double staining with a rabbit fibronectin antibody. To rule out different GFAP antibodies being responsible for the different results, we performed double immunostaining with the rabbit anti-GFAP and the rat anti-GFAP antibodies on the same spinal cord tissues from a new batch of three EphA4-/- mice along with three littermate controls 4 days after dorsal hemisection. The same results were obtained with both antibodies, with reactive GFAP-positive processes at the injury site in a relatively loose network somewhat perpendicular to the lesion edge and nonreactive GFAP-positive processes away from the injury in both *EphA4* mutants and control mice (Fig. 14). Thus, these two antibodies give essentially the same staining pattern and the use of one antibody vs. the other is unlikely to explain the different experimental results in the two studies.

Second, the two studies used different quantification methods. Goldshmit et al quantified the numbers of hyperactive and all astrocytes at the lesion. It is not clear how the "lesion" was defined there. We measured GFAP immunoreactivity at the "lesion core", defined as the GFAP negative area at the center of the original location of the dorsal hemisection, and the "lesion border", defined as the GFAP rich area immediately surrounding the lesion core. We did not use the cell morphology method because we found it rather difficult to reliably pick out individual cell bodies among the thick tangled gliotic structure along the lesion border at 14 days after injury, and that the amount of debris and scattered GFAP positive fragments made identifying astrocyte cell bodies at 4 days also somewhat problematic. Regardless, it is important to realize that there are two distinct areas of the astroglial-fibrotic scar: a largely

GFAP-negative lesion core surrounded by a largely GFAP-positive lesion border, and, accordingly, to analyze these two areas separately.

Third, different lines of mutants were used in the two studies. While Goldshmit et al used an *EphA4* gene targeted mutant (Dottori, et al., 1998), we used an *EphA4* gene trap mutant (Leighton, et al., 2001). Although the two mutations were obtained through different genetic manipulations, they appear to cause the same axon recrossing defects and the same hopping gait, indicating their similar nature as loss-of-function alleles (Dottori, et al., 1998; Leighton, et al., 2001). Fourth, genetic background may contribute to phenotypic variations. In this regard, both mutants have been backcrossed to C57BL/6 for three times or more (Goldshmit, et al., 2004) (and this study). Thus, neither the nature of the mutation nor the genetic background is likely to be a primary factor here. Fifth, the post-injury time points examined in the two studies differ somewhat. While Goldshmit et al focused on the relatively early stage of the astroglial response at 2, 4 and 7 days after injury, our analysis encompassed both an early stage (4 days after injury) and a later, more mature stage of astroglial response (14 days after injury). Nevertheless, both studies had an overlapping time point at 4 days after injury, where the previous study detected a reduction in astroglial response in *EphA4* mutant mice while we did not. Thus, it is unlikely that the different (but overlapping) time points examined in the two studies would explain the different observations.

Finally, and perhaps most importantly, the lesion models employed in the two studies are different. While Goldshmit et al. applied a lateral hemisection model at T12/L1, we used a dorsal hemisection model at T8. The different injury models (lateral vs. dorsal hemisection) and the different locations of the injury (T12/L1 vs. T8) may cause different amounts of damage to the grey vs. white matter and different levels of astroglial response, possibly even from astrocytes of different characteristics. For instance, white matter (fibrous) and grey matter (protoplasmic) astrocytes are known to express different biochemical markers and exhibit different responses to injury (Fang, et al., 2006; Miller and Raff, 1984; Nagy, et al., 1999; Shannon, et al., 2007). It is conceivable that injuries that cause different amount of damage between the white and grey matter may thus lead to a differential response from white vs. grey matter astrocytes. Further work is required to determine whether the different findings in the two *EphA4* mutant studies (Goldshmit, et al., 2004) (and this study) reflect injury type-specific effects of EphA4 on SCI or other aspects of experimental manipulations. At the minimum, the contrast between our study and the previous study by Goldshmit et al illustrates a level of complexity in the astroglial response and astroglial-fibrotic scar formation after SCI that is currently not well understood. Clarifying the role of EphA4 – and Ephrins and Eph receptors in general – in reactive astrogliosis and astroglial-fibrotic scar formation, along with their role in axonal growth after SCI, is crucial for any therapeutic development for SCI by targeting the promiscuous EphA4 or the Ephrin/Eph signaling pathway.

Acknowledgments

REFERENCES

Bradbury EJ, Moon LD, Popat RJ, King VR, Bennett GS, Patel PN, Fawcett JW, McMahon SB. Chondroitinase ABC promotes functional recovery after spinal cord injury. Nature 2002;416:636–640. [PubMed: 11948352]

Brambilla R, Bracchi-Ricard V, Hu WH, Frydel B, Bramwell A, Karmally S, Green EJ, Bethea JR. Inhibition of astroglial nuclear factor kappaB reduces inflammation and improves functional recovery after spinal cord injury. J Exp Med 2005;202:145–156. [PubMed: 15998793]

Bundesen LQ, Scheel TA, Bregman BS, Kromer LF. Ephrin-B2 and EphB2 regulation of astrocyte-meningeal fibroblast interactions in response to spinal cord lesions in adult rats. J Neurosci 2003;23:7789–7800. [PubMed: 12944508]

Cheng HJ, Nakamoto M, Bergemann AD, Flanagan JG. Complementary gradients in expression and binding of ELF-1 and Mek4 in development of the topographic retinotectal projection map. Cell 1995;82:371–381. [PubMed: 7634327]

Cruz-Orengo L, Figueroa JD, Torrado A, Puig A, Whittemore SR, Miranda JD. Reduction of EphA4 receptor expression after spinal cord injury does not induce axonal regeneration or return of tcMMEP response. Neurosci Lett 2007;418:49–54. [PubMed: 17418490]

Cruz-Orengo L, Figueroa JD, Velazquez I, Torrado A, Ortiz C, Hernandez C, Puig A, Segarra AC, Whittemore SR, Miranda JD. Blocking EphA4 upregulation after spinal cord injury results in enhanced chronic pain. Exp Neurol 2006;202:421–433. [PubMed: 16959251]

Davies SJ, Goucher DR, Doller C, Silver J. Robust regeneration of adult sensory axons in degenerating white matter of the adult rat spinal cord. J Neurosci 1999;19:5810–5822. [PubMed: 10407022]

Dottori M, Hartley L, Galea M, Paxinos G, Polizzotto M, Kilpatrick T, Bartlett PF, Murphy M, Kontgen F, Boyd AW. EphA4 (Sek1) receptor tyrosine kinase is required for the development of the corticospinal tract. Proc Natl Acad Sci U S A 1998;95:13248–13253. [PubMed: 9789074]

Fabes J, Anderson P, Brennan C, Bolsover S. Regeneration-enhancing effects of EphA4 blocking peptide following corticospinal tract injury in adult rat spinal cord. Eur J Neurosci 2007;26:2496–2505. [PubMed: 17970742]

Fabes J, Anderson P, Yanez-Munoz RJ, Thrasher A, Brennan C, Bolsover S. Accumulation of the inhibitory receptor EphA4 may prevent regeneration of corticospinal tract axons following lesion. Eur J Neurosci 2006;23:1721–1730. [PubMed: 16623828]

Fang Z, Duthoit N, Wicher G, Kallskog O, Ambartsumian N, Lukanidin E, Takenaga K, Kozlova EN. Intracellular calcium-binding protein S100A4 influences injury-induced migration of white matter astrocytes. Acta Neuropathol 2006;111:213–219. [PubMed: 16463066]

Faulkner JR, Herrmann JE, Woo MJ, Tansey KE, Doan NB, Sofroniew MV. Reactive astrocytes protect tissue and preserve function after spinal cord injury. J Neurosci 2004;24:2143–2155. [PubMed: 14999065]

Fawcett JW, Asher RA. The glial scar and central nervous system repair. Brain Res Bull 1999;49:377–391. [PubMed: 10483914]

Fitch MT, Silver J. CNS injury, glial scars, and inflammation: Inhibitory extracellular matrices and regeneration failure. Exp Neurol 2008;209:294–301. [PubMed: 17617407]

Goldshmit Y, Galea MP, Wise G, Bartlett PF, Turnley AM. Axonal regeneration and lack of astrocytic gliosis in EphA4-deficient mice. J Neurosci 2004;24:10064–10073. [PubMed: 15537875]

Grossman SD, Rosenberg LJ, Wrathall JR. Temporal-spatial pattern of acute neuronal and glial loss after spinal cord contusion. Exp Neurol 2001;168:273–282. [PubMed: 11259115]

Hausmann ON. Post-traumatic inflammation following spinal cord injury. Spinal Cord 2003;41:369–378. [PubMed: 12815368]

Herrmann JE, Imura T, Song B, Qi J, Ao Y, Nguyen TK, Korsak RA, Takeda K, Akira S, Sofroniew MV. STAT3 is a critical regulator of astrogliosis and scar formation after spinal cord injury. J Neurosci 2008;28:7231–7243. [PubMed: 18614693]

Herrmann JE, Pence MA, Shapera EA, Shah RR, Geoffroy CG, Zheng B. Generation of an *EphA4* conditional allele in mice. Genesis. 2009 In press.

Inman D, Guth L, Steward O. Genetic influences on secondary degeneration and wound healing following spinal cord injury in various strains of mice. J Comp Neurol 2002;451:225–235. [PubMed: 12210135]

Irizarry-Ramirez M, Willson CA, Cruz-Orengo L, Figueroa J, Velazquez I, Jones H, Foster RD, Whittemore SR, Miranda JD. Upregulation of EphA3 receptor after spinal cord injury. J Neurotrauma 2005;22:929–935. [PubMed: 16083359]

Klapka N, Muller HW. Collagen matrix in spinal cord injury. J Neurotrauma 2006;23:422–435. [PubMed: 16629627]

Kullander K, Butt SJ, Lebret JM, Lundfald L, Restrepo CE, Rydstrom A, Klein R, Kiehn O. Role of EphA4 and EphrinB3 in local neuronal circuits that control walking. Science 2003;299:1889–1892. [PubMed: 12649481]

Kuno R, Yoshida Y, Nitta A, Nabeshima T, Wang J, Sonobe Y, Kawanokuchi J, Takeuchi H, Mizuno T, Suzumura A. The role of TNF-alpha and its receptors in the production of NGF and GDNF by astrocytes. Brain Res 2006;1116:12–18. [PubMed: 16956589]

Lee JK, Chan AF, Luu SM, Zhu Y, Ho C, Tessier-Lavigne M, Zheng B. Reassessment of corticospinal tract regeneration in Nogo-deficient mice. J Neurosci 2009;29:8649–8654. [PubMed: 19587271]

Leighton PA, Mitchell KJ, Goodrich LV, Lu X, Pinson K, Scherz P, Skarnes WC, Tessier-Lavigne M. Defining brain wiring patterns and mechanisms through gene trapping in mice. Nature 2001;410:174–179. [PubMed: 11242070]

Liu XZ, Xu XM, Hu R, Du C, Zhang SX, McDonald JW, Dong HX, Wu YJ, Fan GS, Jacquin MF, Hsu CY, Choi DW. Neuronal and glial apoptosis after traumatic spinal cord injury. J Neurosci 1997;17:5395–5406. [PubMed: 9204923]

Ma M, Basso DM, Walters P, Stokes BT, Jakeman LB. Behavioral and histological outcomes following graded spinal cord contusion injury in the C57Bl/6 mouse. Exp Neurol 2001;169:239–254. [PubMed: 11358439]

Miller RH, Raff MC. Fibrous and protoplasmic astrocytes are biochemically and developmentally distinct. J Neurosci 1984;4:585–592. [PubMed: 6366155]

Miranda JD, White LA, Marcillo AE, Willson CA, Jagid J, Whittemore SR. Induction of Eph B3 after spinal cord injury. Exp Neurol 1999;156:218–222. [PubMed: 10192794]

Nagy JI, Patel D, Ochalski PA, Stelmack GL. Connexin30 in rodent, cat and human brain: selective expression in gray matter astrocytes, co-localization with connexin43 at gap junctions and late developmental appearance. Neuroscience 1999;88:447–468. [PubMed: 10197766]

Nguyen KA, Santos SJ, Kreidel MK, Diaz AL, Rey R, Lawson MA. Acute regulation of translation initiation by gonadotropin-releasing hormone in the gonadotrope cell line LbetaT2. Mol Endocrinol 2004;18:1301–1312. [PubMed: 14752057]

Niclou SP, Ehlert EM, Verhaagen J. Chemorepellent axon guidance molecules in spinal cord injury. J Neurotrauma 2006;23:409–421. [PubMed: 16629626]

Norenberg MD, Smith J, Marcillo A. The pathology of human spinal cord injury: defining the problems. J Neurotrauma 2004;21:429–440. [PubMed: 15115592]

Norton WT, Aquino DA, Hozumi I, Chiu FC, Brosnan CF. Quantitative aspects of reactive gliosis: a review. Neurochem Res 1992;17:877–885. [PubMed: 1407275]

Okada S, Nakamura M, Katoh H, Miyao T, Shimazaki T, Ishii K, Yamane J, Yoshimura A, Iwamoto Y, Toyama Y, Okano H. Conditional ablation of Stat3 or Socs3 discloses a dual role for reactive astrocytes after spinal cord injury. Nat Med 2006;12:829–834. [PubMed: 16783372]

Orioli D, Henkemeyer M, Lemke G, Klein R, Pawson T. Sek4 and Nuk receptors cooperate in guidance of commissural axons and in palate formation. EMBO J 1996;15:6035–6049. [PubMed: 8947026]

Pasquale EB. Eph-ephrin bidirectional signaling in physiology and disease. Cell 2008;133:38–52. [PubMed: 18394988]

Plemel JR, Duncan G, Chen KW, Shannon C, Park S, Sparling JS, Tetzlaff W. A graded forceps crush spinal cord injury model in mice. J Neurotrauma 2008;25:350–370. [PubMed: 18373484]

Shannon C, Salter M, Fern R. GFP imaging of live astrocytes: regional differences in the effects of ischaemia upon astrocytes. J Anat 2007;210:684–692. [PubMed: 17523937]

Shearer MC, Fawcett JW. The astrocyte/meningeal cell interface--a barrier to successful nerve regeneration? Cell Tissue Res 2001;305:267–273. [PubMed: 11545264]

Silver J, Miller JH. Regeneration beyond the glial scar. Nat Rev Neurosci 2004;5:146–156. [PubMed: 14735117]

Skarnes WC, Moss JE, Hurtley SM, Beddington RS. Capturing genes encoding membrane and secreted proteins important for mouse development. Proc Natl Acad Sci U S A 1995;92:6592–6596. [PubMed: 7604039]

Sofroniew MV. Molecular dissection of reactive astrogliosis and glial scar formation. Trends Neurosci. 2009

Sroga JM, Jones TB, Kigerl KA, McGaughy VM, Popovich PG. Rats and mice exhibit distinct inflammatory reactions after spinal cord injury. J Comp Neurol 2003;462:223–240. [PubMed: 12794745]

Voskuhl RR, Peterson RS, Song B, Ao Y, Morales LB, Tiwari-Woodruff S, Sofroniew MV. Reactive astrocytes form scar-like perivascular barriers to leukocytes during adaptive immune inflammation of the CNS. J Neurosci 2009;29:11511–11522. [PubMed: 19759299]

Wang HU, Anderson DJ. Eph family transmembrane ligands can mediate repulsive guidance of trunk neural crest migration and motor axon outgrowth. Neuron 1997;18:383–396. [PubMed: 9115733]

Wang X, Messing A, David S. Axonal and nonneuronal cell responses to spinal cord injury in mice lacking glial fibrillary acidic protein. Exp Neurol 1997;148:568–576. [PubMed: 9417833]

Willson CA, Irizarry-Ramirez M, Gaskins HE, Cruz-Orengo L, Figueroa JD, Whittemore SR, Miranda JD. Upregulation of EphA receptor expression in the injured adult rat spinal cord. Cell Transplant 2002;11:229–239. [PubMed: 12075988]

Willson CA, Miranda JD, Foster RD, Onifer SM, Whittemore SR. Transection of the adult rat spinal cord upregulates EphB3 receptor and ligand expression. Cell Transplant 2003;12:279–290. [PubMed: 12797382]

Yaron A, Zheng B. Navigating their way to the clinic: Emerging roles for axon guidance molecules in neurological disorders and injury. Dev Neurobiol. 2007

Zhang Z, Fujiki M, Guth L, Steward O. Genetic influences on cellular reactions to spinal cord injury: a wound-healing response present in normal mice is impaired in mice carrying a mutation (WldS) that causes delayed Wallerian degeneration. J Comp Neurol 1996;371:485–495. [PubMed: 8842901]

Zheng B, Atwal J, Ho C, Case L, He XL, Garcia KC, Steward O, Tessier-Lavigne M. Genetic deletion of the Nogo receptor does not reduce neurite inhibition in vitro or promote corticospinal tract regeneration in vivo. Proc Natl Acad Sci U S A 2005;102:1205–1210. [PubMed: 15647357]

Zheng B, Lee JK, Xie F. Genetic mouse models for studying inhibitors of spinal axon regeneration. Trends Neurosci 2006;29:640–646. [PubMed: 17030430]
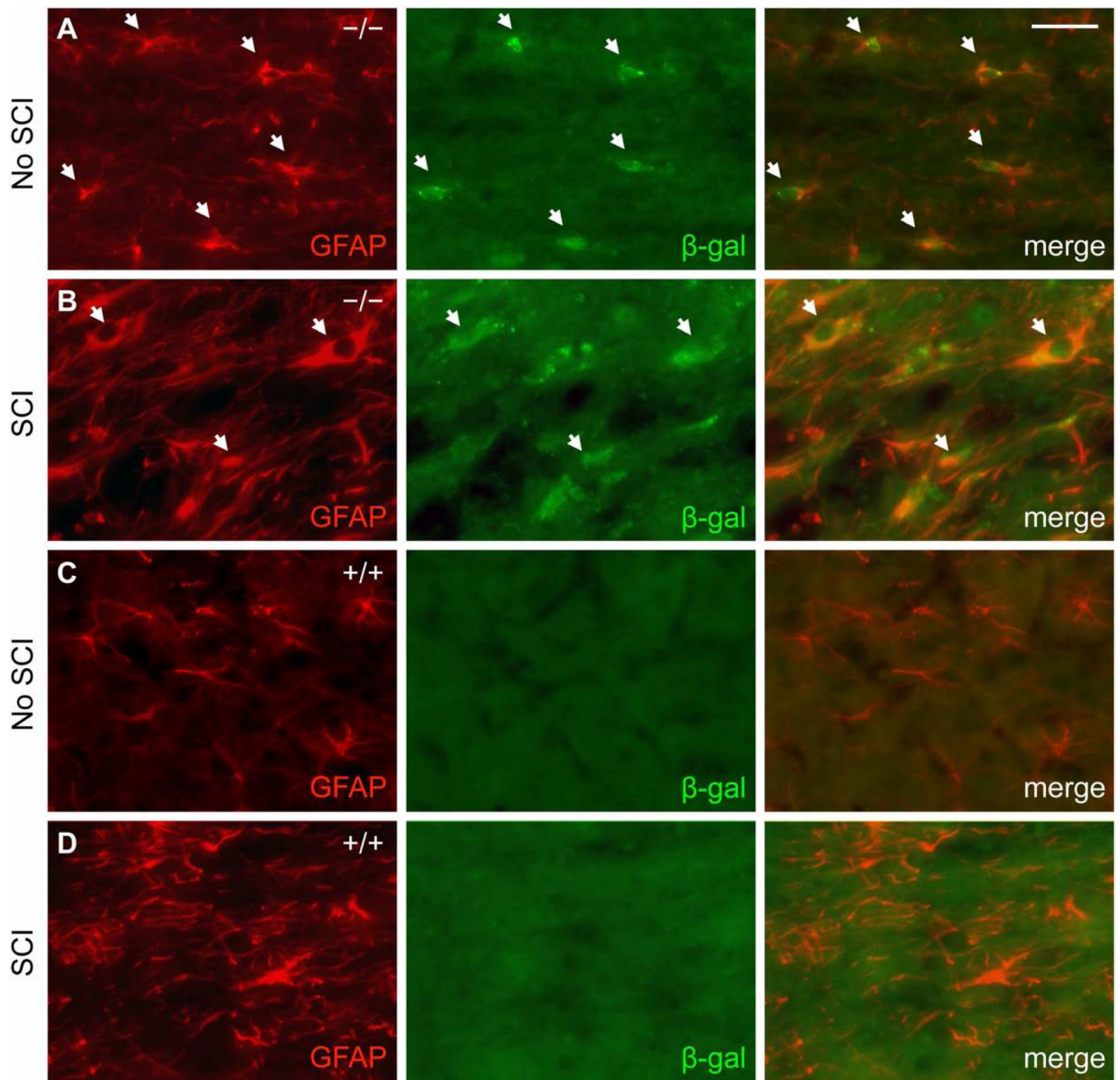
Fig. 1.
β-gal reporter expression in EphA4−/− mice predominantly co-localizes with GFAP-positive cells in the spinal cord before and after dorsal hemisection SCI. GFAP (red) and β-gal (green) immunoreactivity from representative EphA4−/− (A, B) and wild type control (C, D) mice is shown on sagittal sections in the grey matter close to the injury site (within ~200 μm of the lesion core) 14 days after SCI (B, D) or in a comparable area without SCI (A, C). White arrows in (A, B) indicate examples of cells immunoreactive for both GFAP and β-gal. Scale bar = 40 μm.
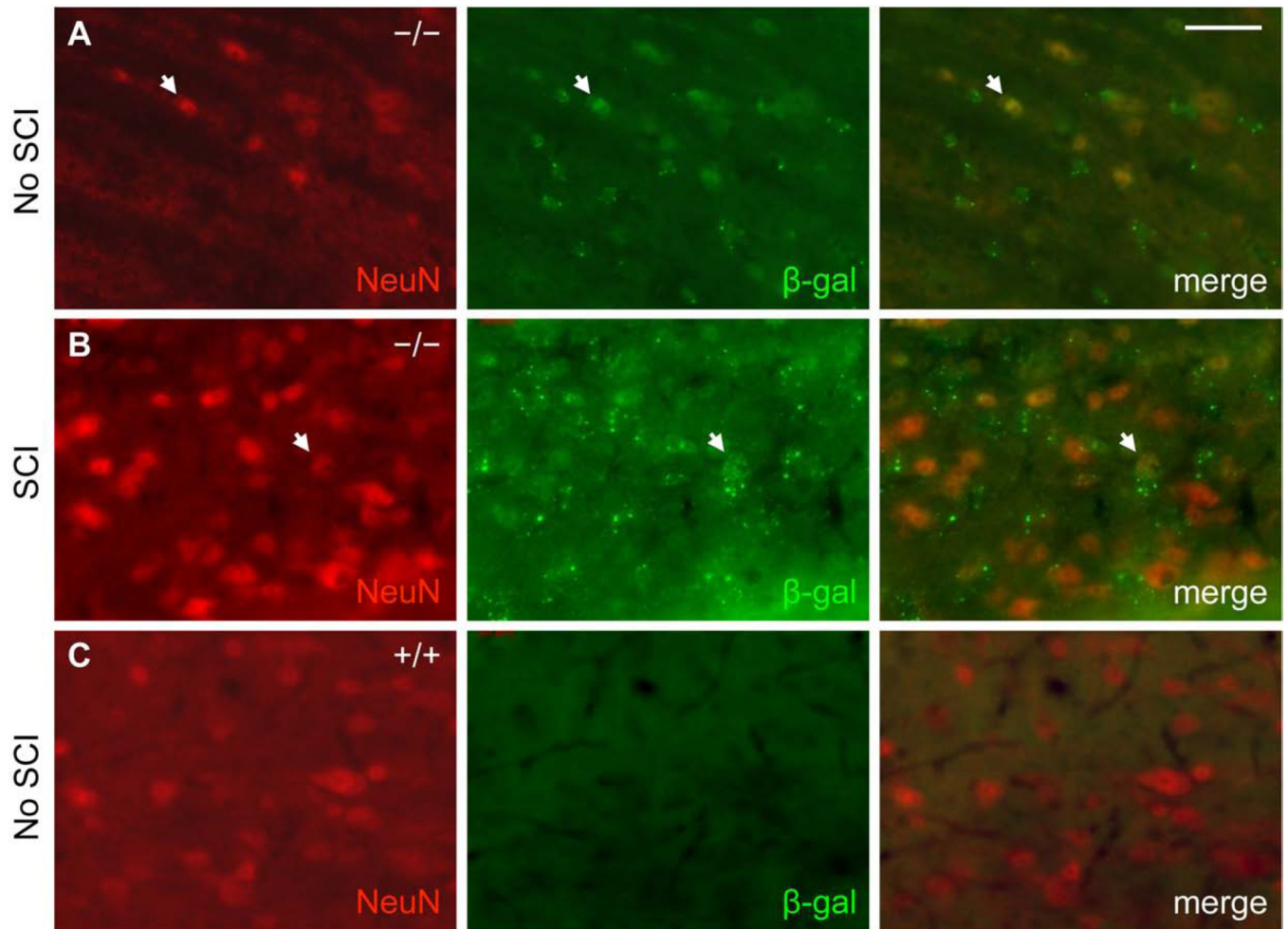
Fig. 2.
A subset of β-gal expressing cells in EphA4−/− mice co-stain with NeuN in the spinal cord before and after SCI. NeuN (red) and β-gal (green) immunoreactivity from representative EphA4−/− (A, B) and wild type control (C) mice is shown on sagittal sections in the grey matter close to the injury site (within ~200 μm of the lesion core) 14 days after SCI (B) or in a comparable area without SCI (A, C). Scale bar = 40 μm.
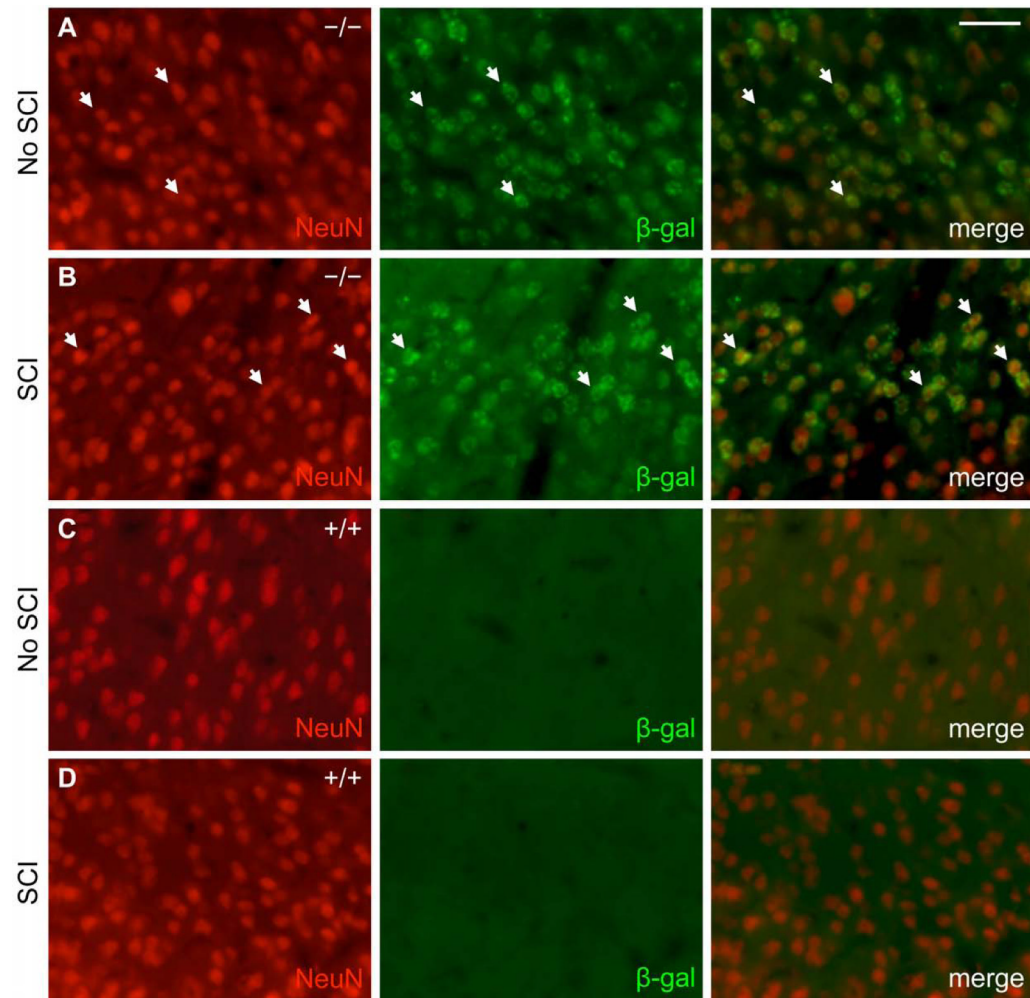
Fig. 3.
β-gal reporter expression extensively co-localizes with neuronal marker NeuN in the sensorimotor cortex of adult mice. NeuN (red) and β-gal (green) immunoreactivity from representative EphA4−/− (A, B) and wild type control (C, D) mice is shown on coronal sections of the sensorimotor cortex without (A, C) or 14 days after SCI (B, D). Scale bar = 40 μm.
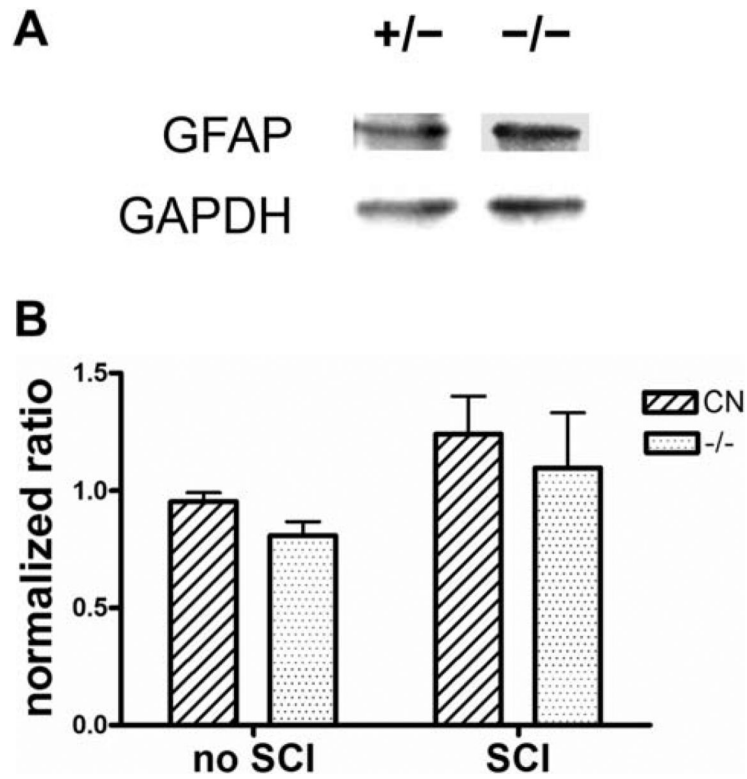
Fig. 4.
Western blot of GFAP expression in early phases following dorsal hemisection SCI. (A)
Representative Western Blot on injured spinal cord from EphA4+/- and EphA4−/− mice. (B)
Quantification of western blot. Signal intensity for each band was first converted to peaks and
the area underneath each peak was then calculated. For each sample, GFAP signal is first
normalized against the GAPDH loading control, and then the resulting ratio is further
normalized against that of a control animal run on all blots, which is plotted as the "normalized
ratio" (Nguyen, et al., 2004). CN, control. n ≥ 3 per group. No statistically significant
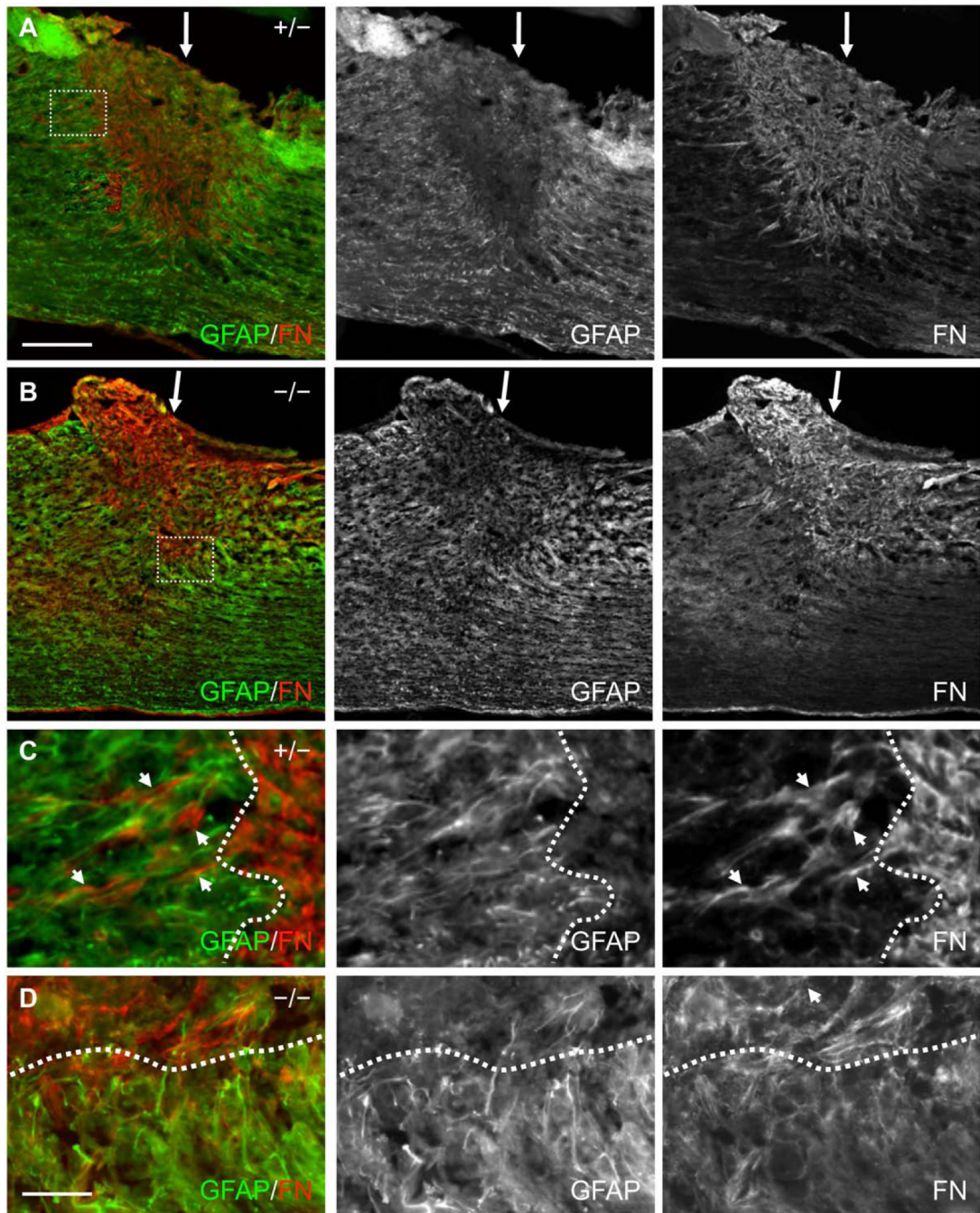differences between EphA4+/- and EphA4−/− mice as determined by two-way ANOVA.
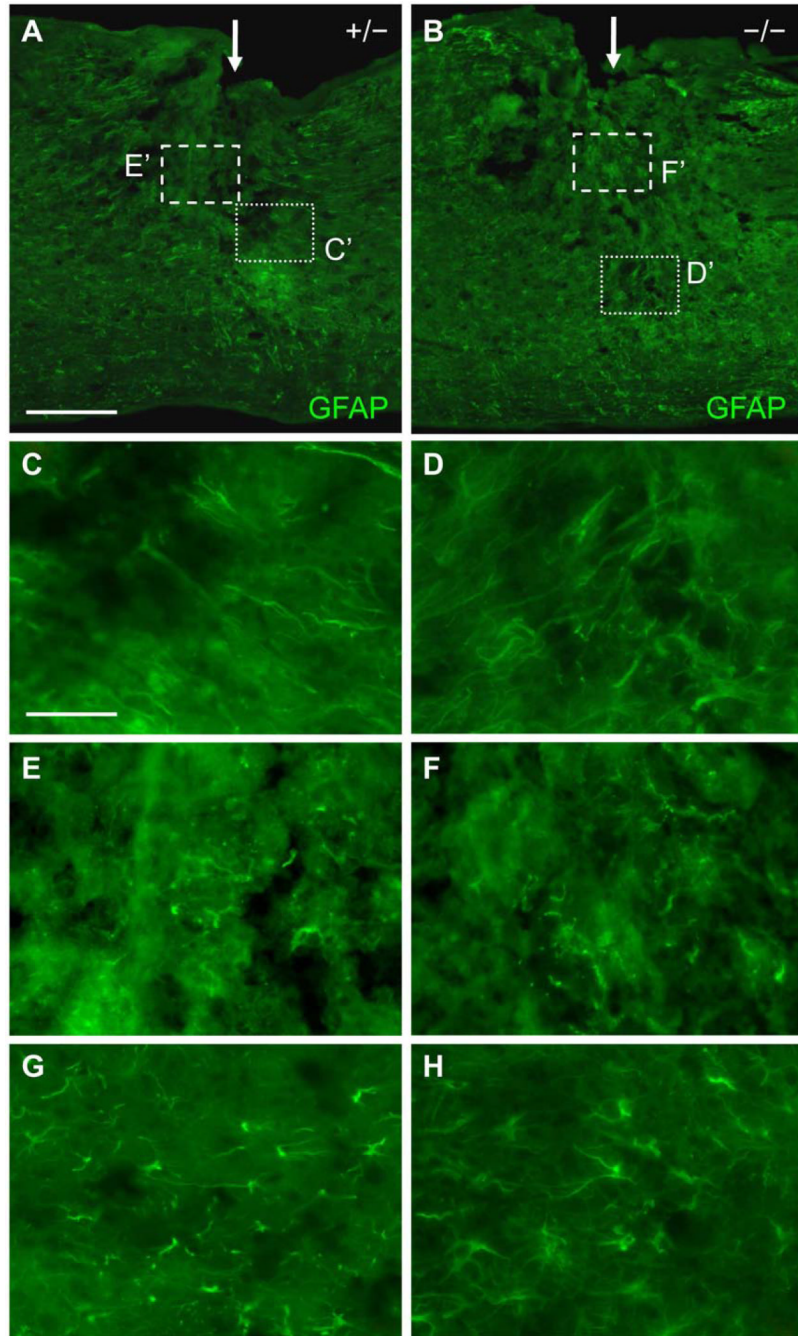
Fig. 5.
GFAP immunoreactivity in the spinal cord of EphA4+/- and EphA4−/− mice 4 days after SCI. (A, B) Lower magnification sagittal view of GFAP expression at the dorsal hemisection injury site (indicated by a white arrow) in a representative EphA4+/- (A) or EphA4−/− (B) mouse. (C, D) Higher magnification view of the dotted box in (A, B) respectively showing similar morphology and disorientation of GFAP-positive processes along the lesion border in EphA4 +/- (C) and EphA4−/− (D) mice. (E, F) Higher magnification view of the dashed box in (A, B) respectively showing the similar pattern of scattered GFAP-positive processes and debris in the center of the lesion in EphA4+/- (E) and EphA4−/− (F) mice. (G, H) Higher magnification

images of GFAP-positive cells ~400 μm from the lesion core, showing similar morphology between EphA4+/- (G) and EphA4−/− (H) mice. Scale bar = 300 μm (A, B); 60 μm (C-H).
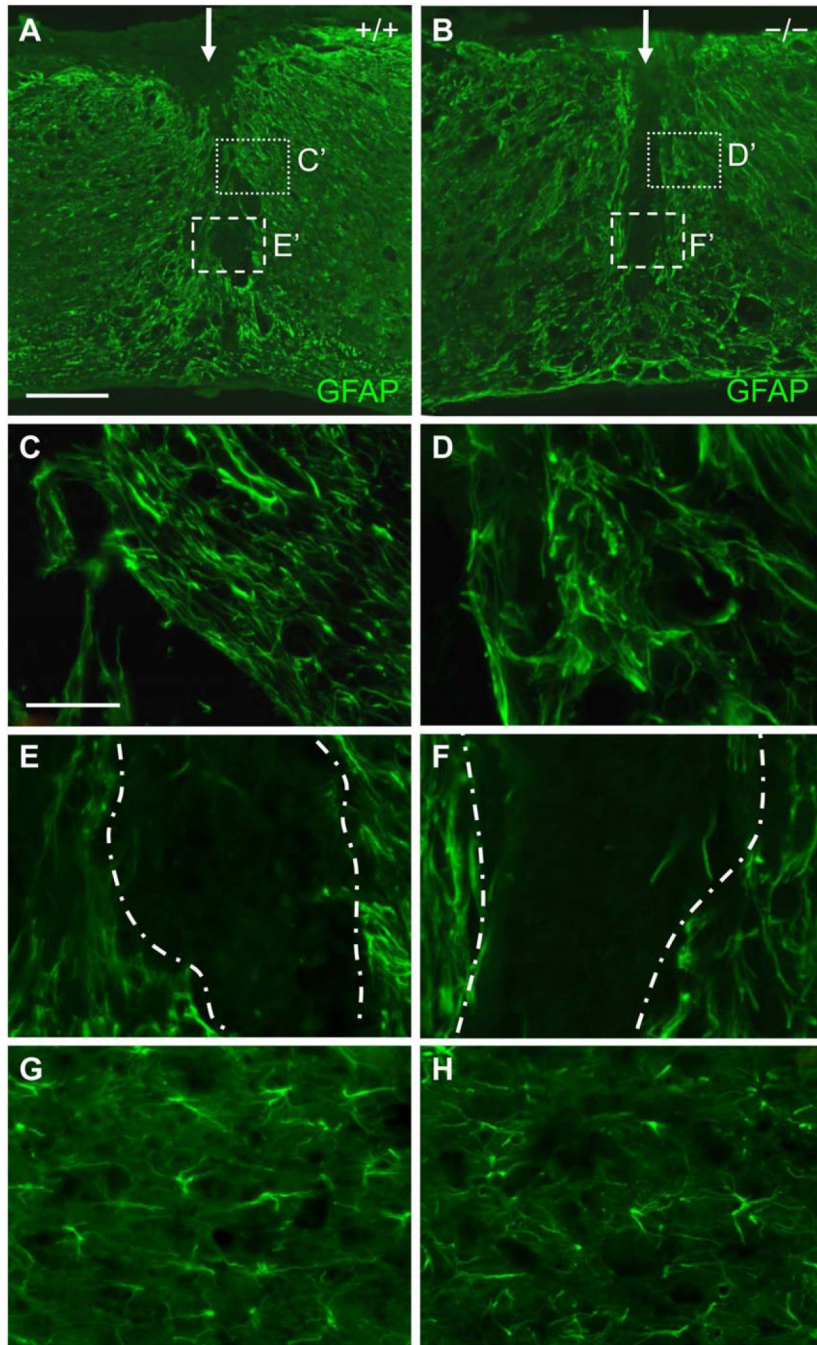
Fig. 6.
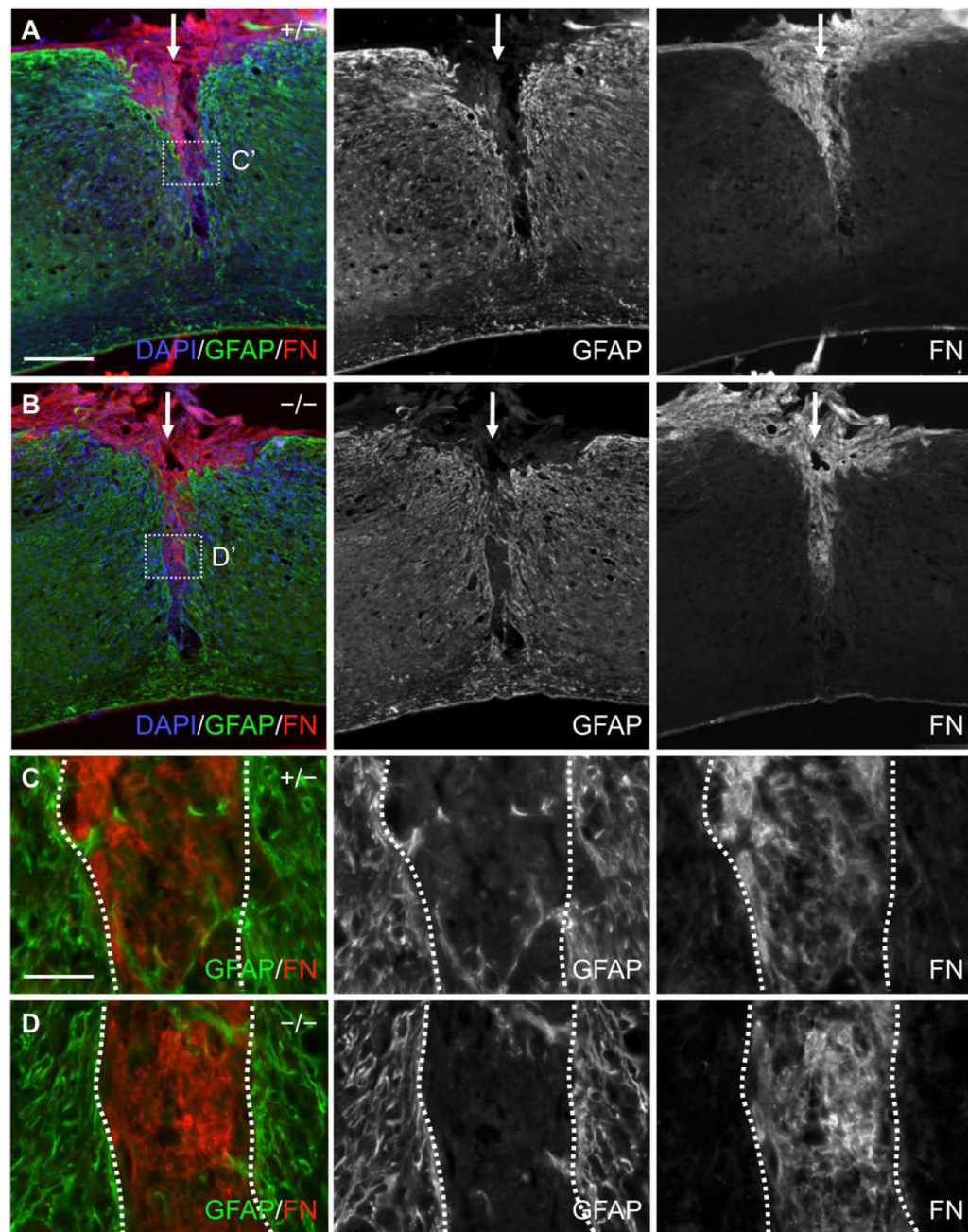GFAP immunoreactivity in the spinal cord of EphA4+/- and EphA4−/− mice 14 days after SCI. (A, B) Lower magnification sagittal view of GFAP expression at the dorsal hemisection injury site (indicated by a white arrow) in a representative EphA4+/+ (A) or EphA4−/− (B) mouse. Note a much clearer border between largely GFAP-positive cells and the largely GFAP-negative lesion core in both (A) and (B), as compared to Fig. 5A and B. (C, D) High magnification view of the dotted boxes in (A) and (B) respectively, showing alignment of GFAP-positive cells/processes parallel to the lesion edge in both EphA4+/+ (C) and EphA4−/− (D) mice. (E, F) Higher magnification view of the dashed boxes in (A) and (B) respectively, showing the largely GFAP-negative lesion core. Lesion edges are demarcated with dash-dot

lines. Note the similar pattern of overall low level of GFAP expression in the lesion core that contains few GFAP-positive processes in control (E) and mutant (F) mice. (G, H) Higher magnification images of GFAP-positive cells ~400 μm from the lesion core, showing similar morphology between EphA4+/+ (G) and EphA4−/− (H) mice. Scale bar = 300 μm (A, B); 60 μm (C-H).
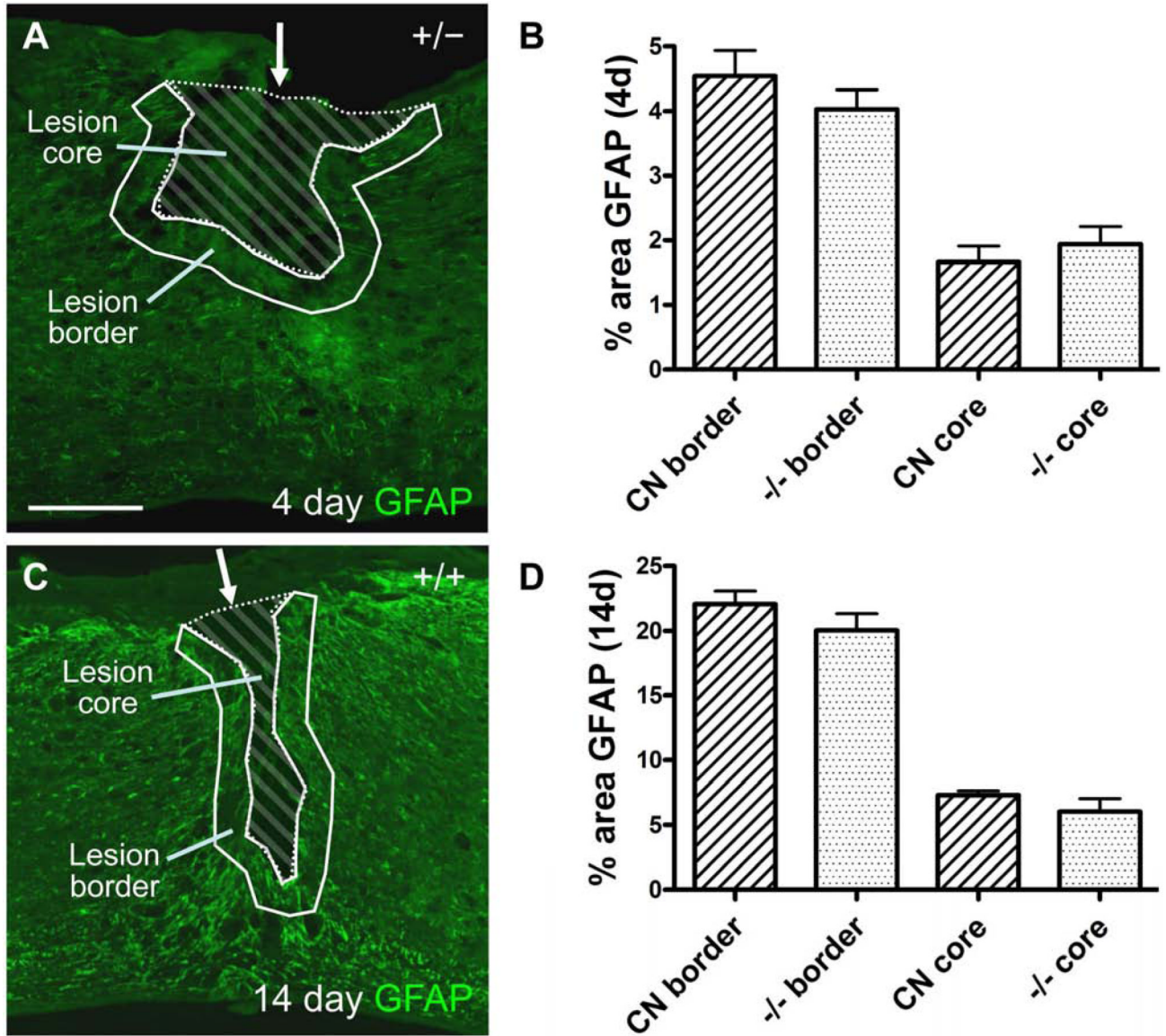
Fig. 7.
Quantification of GFAP immunoreactivity after SCI. (A, C) Examples of the lesion area at 4 (A) or 14 (C) days after SCI. Solid lines mark the lesion border, which is an area 100 μm outward from the low GFAP immunoreactive lesion core. Striped areas within the lesion border indicate the lesion core. Scale bar = 300 μm. (B, D) Quantification of percent area of GFAP immunoreactivity within the 100 μm wide lesion border or the lesion core 4 (B) and 14 (D) days after SCI. No statistically significant differences exist between control and EphA4−/− groups for any measure ($P > 0.05$, two tailed t-test). CN, control. n = 8 (control, 4 days); 6 (EphA4−/−, 4 days); 12 (control, 14 days); 9 (EphA4−/−, 14 days).

Fig. 8.
Fibronectin and GFAP immunoreactivity in the spinal cord of EphA4+/− and EphA4−/− mice 4 days after SCI. (A, B) Lower magnification sagittal view of GFAP (green) and fibronectin (FN, red) immunoreactivity at the dorsal hemisection injury site (indicated by a white arrow) in a representative EphA4+/− (A) or EphA4−/− (B) mouse. Note that the lesion edge was not yet fully defined and there was noticeable intermingling of GFAP-positive and fibronectin-positive cells/processes around the lesion border in both genotypes. (C, D) Higher magnification view of the dotted box in (A) and (B) respectively showing intermingling of fibronectin-positive cells/processes with GFAP-positive processes around the lesion edge

(dotted line) as the astroglial-meningeal scar border began to form in both genotypes. Scale bar = 300 μm (A, B); 50 μm (C, D).

Fig. 9.
Fibronectin and GFAP immunoreactivity in the spinal cord of EphA4+/− and EphA4−/− mice 14 days after SCI. (A, B) Lower magnification sagittal view of GFAP (green) and fibronectin (FN, red) immunoreactivity at the dorsal hemisection injury site (indicated by a white arrow) in a representative EphA4+/− (A) or EphA4−/− (B) mouse. DAPI counterstain (in blue) indicates the presence of numerous cells at the lesion core. Note the much more clearly defined lesion edge in both genotypes at this time point as compared to 4 days after SCI in Figure 8A and B. (C, D) Higher magnification view of the dotted box from (A) and (B) respectively showing some intermingling of GFAP-positive processes into the fibronectin-dense lesion core, but only faint fibronectin immunoreactivity (but not strong fibronectin-positive cells/

processes) in the GFAP-dense lesion rim in both genotypes. Dotted lines demarcate lesion edges; lesion core is between the two dotted lines. Scale bar = 300 μm (A, B); 50 μm (C, D).
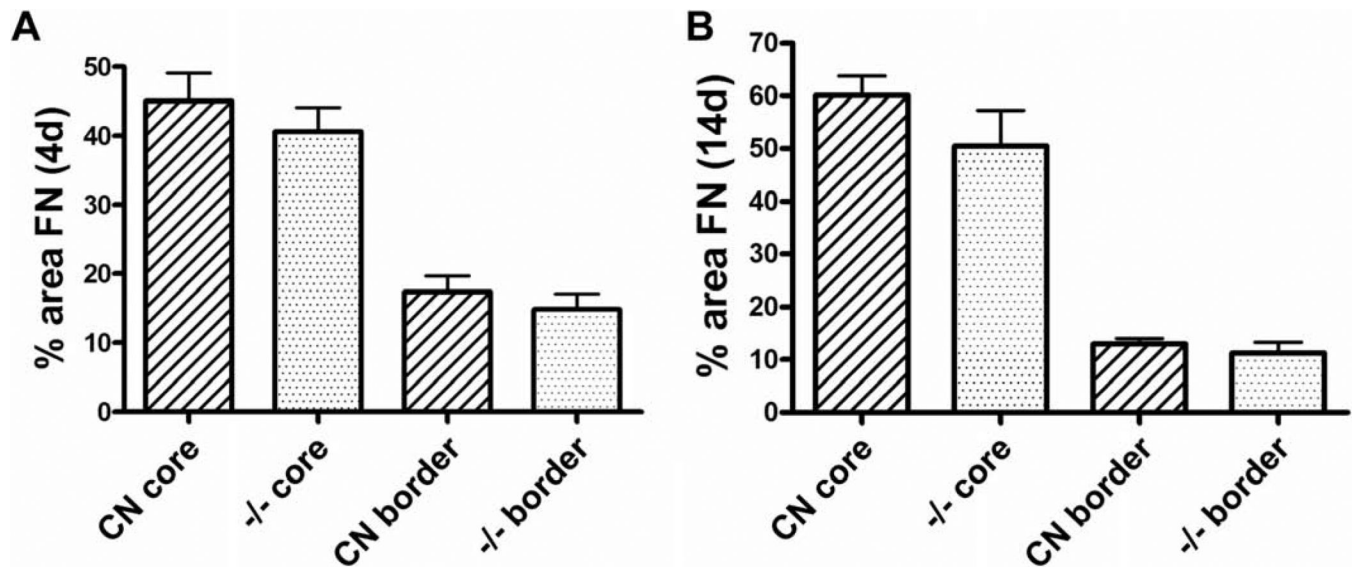
Fig. 10.
Quantification of fibronectin immunoreactivity after SCI. The same scheme was used to define lesion core and lesion border as in Figure 7. FN, fibronectin. Fibronectin-positive pixels/unit area within the lesion core and lesion border was quantified. (A) 4 days after SCI. n = 8 (controls); 6 (EphA4−/−). (B) 14 days after SCI. n = 12 (controls); 10 (EphA4−/−). CN, control. No statistically significant differences between controls and EphA4−/− mice in any measure ($P > 0.05$, Student's *t*-test).
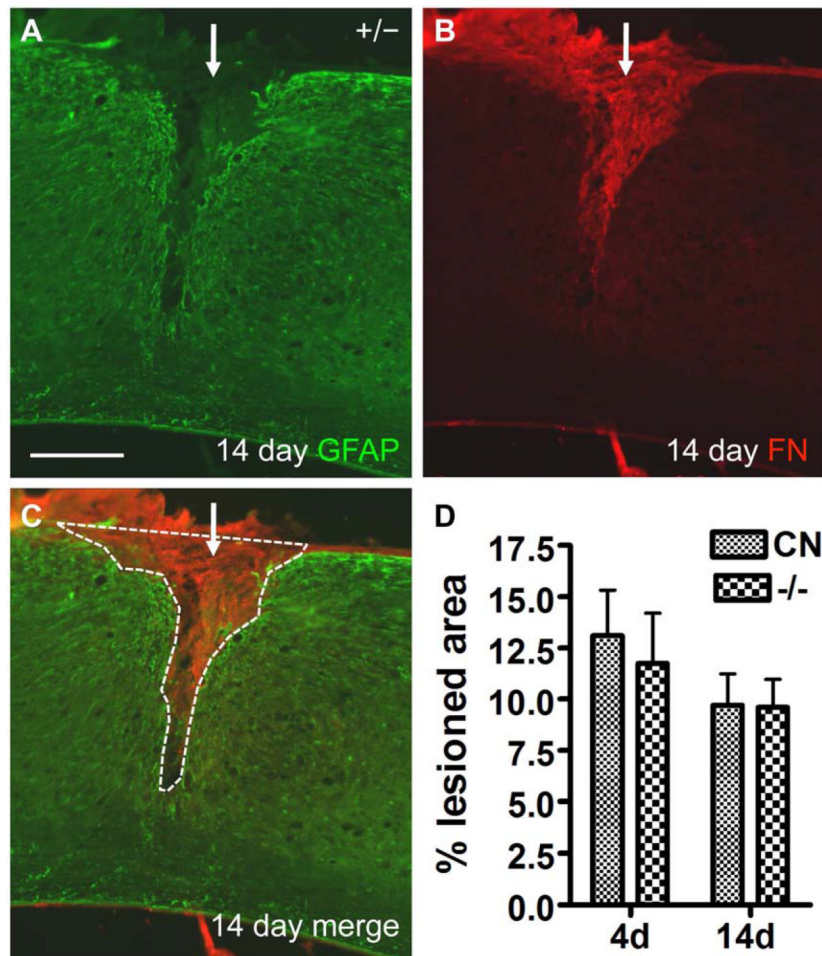
Fig. 11.
Lesion size was not significantly different between control and EphA4−/− mice at 4 or 14 days after SCI. (A-C) Example of GFAP and fibronectin (FN) immunoreactivity of the injury site in a control mouse 14 days after SCI. Note the largely GFAP-negative area at the lesion core, which closely matches the fibronectin-positive staining. White dashed line around GFAP-negative core demarcates the lesion area measured, which was then normalized against the height of the spinal cord. Scale bar = 300 μm. (D) Graph of percent lesion areas at 4 and 14 days after SCI. CN, control. No statistically significant differences were found between groups at either time point (two way ANOVA). n = 6 (control or EphA4−/−, 4 days); 9 (control, 14 days); 8 (EphA4−/−, 14 days).
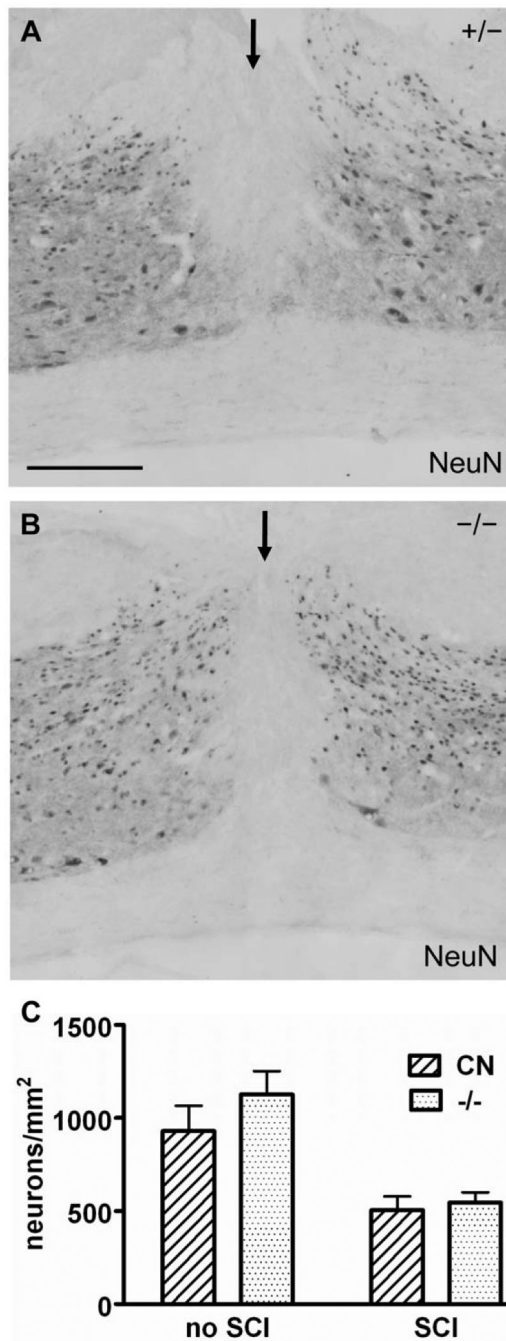
Fig. 12.
Neuronal density was not statistically different between control and EphA4−/− mice after SCI. (A-B) NeuN immunohistochemistry on sagittal sections of the injured cord from representative EphA4+/− (A) or EphA4−/− (B) mice 14 days after SCI. The injury site is indicated by an arrow. Scale bar = 300 μm. (C) Quantification of NeuN immunoreactive neuronal density without or at 14 days after SCI. CN, control. No statistically significant differences in neuronal density between control and EphA4−/− mice were detected without SCI or 14 days after SCI. (*P* > 0.05, Student' *t*-test). n = 3 (uninjured mice/genotype); 4 (injured mice/genotype).
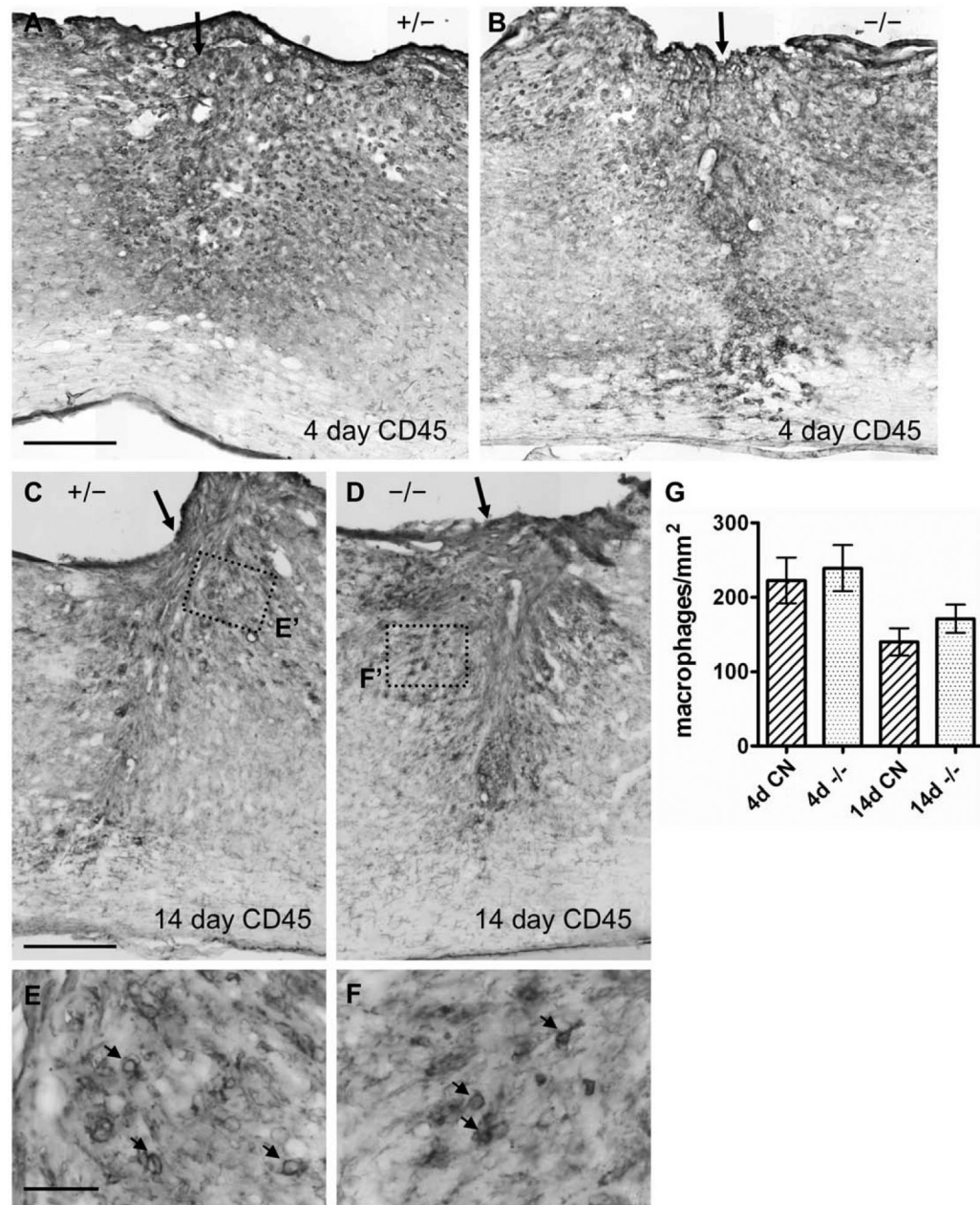
Fig. 13.
Inflammatory response as assessed by a macrophage marker did not differ between control and EphA4−/− mice after SCI. (A-D) Lower magnification view of CD45 macrophage marker immunohistochemistry on spinal cord sagittal sections 4 (A, B) and 14 days (C, D) after SCI in representative EphA4+/− (A, C) or EphA4−/− (B, D) mice. Arrow indicates injury site. (E, F) Higher magnification view of the dotted box in (C) and (D) respectively highlighting CD45-positive macrophages (indicated by arrows) near the lesion site. Scale bar = 300 μm (A-D); 40 μm (E, F). (G) Quantification of CD45-positive macrophages within a rectangular area 1.5 mm long centered around the injury site. CN, control. No statistically significant differences were found with two-way ANOVA. n = 6 - 7/genotype/timepoint.
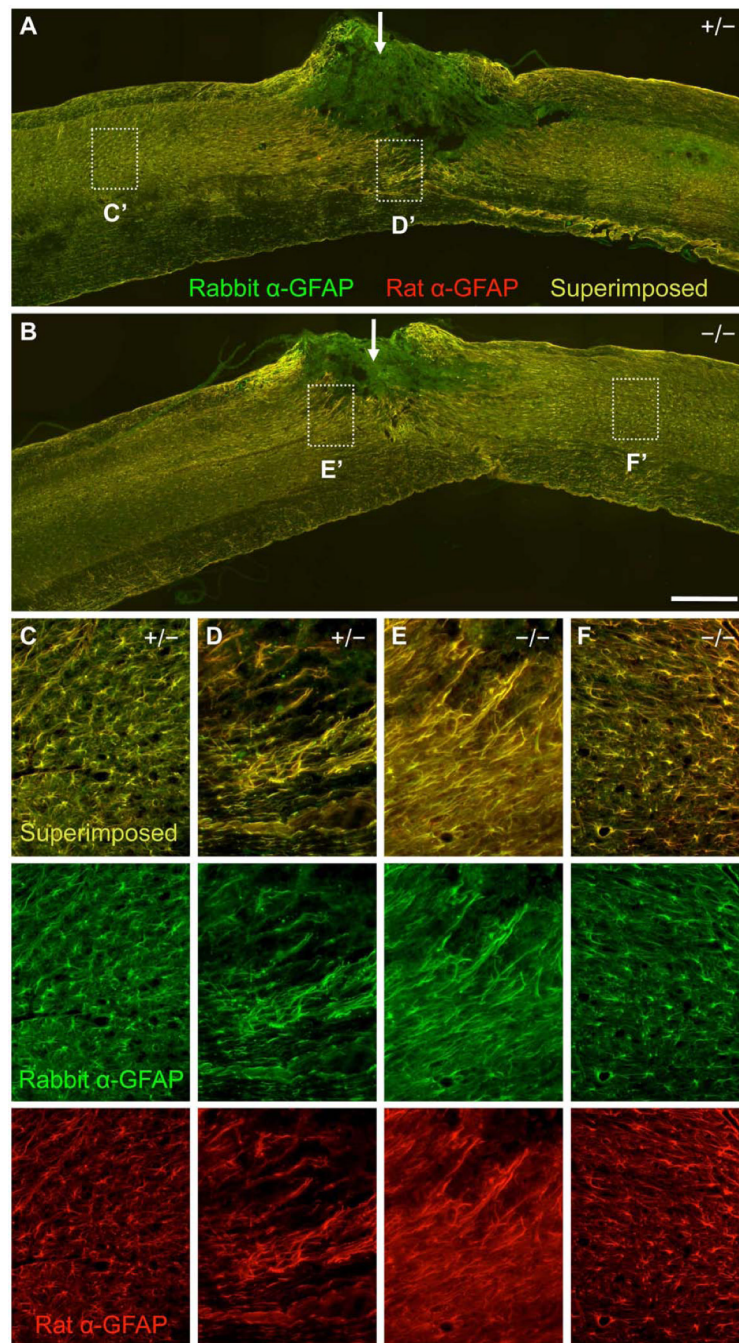
Fig. 14.
Comparison of two different GFAP antibodies for immunohistochemistry on spinal cord tissues 4 days after dorsal hemisection. (A, B) Lower magnification sagittal view of the spinal cord tissue surrounding the dorsal hemisection injury site (indicated by a white arrow) doubly immunostained with rabbit anti-GFAP (in green) and rat anti-GFAP (in red) in a representative EphA4+/− (A) or EphA4−/− (B) mouse (at 6 months of age when injured). Note that the rabbit and rat antibodies give largely the same staining pattern (as indicated by the overlapping, yellowish signals), except at the injury site. The stronger staining intensity for the rabbit anti-GFAP antibody (green color conferred by the secondary antibody) at the injury site is due to a higher background with this primary antibody (under the experimental conditions applied

here) because reversing the color of the secondary antibodies led to a stronger staining intensity for the red channel instead at the injury site (data not shown). (C-F) Higher magnification view of the dotted box from (A) and (B) showing reactive astrocytes at the lesion border (D, E) and non-reactive astrocytes (C, F) away from the injury site in the EphA4+/− (C, D) or EphA4−/− (E, F) mouse. Upper panels: merged images; lower panels: images with rabbit anti-GFAP or rat anti-GFAP alone. Note that the two antibodies gave similar staining patterns, and that the GFAP-positive processes of reactive astrocytes run somewhat perpendicular to the lesion edge in these animals (D, E). Scale bar = 500 μm (A, B); 125 μm (C-F).